Anti-corrosion efficiency of Arum italicum root extracts, green synthesis of silver oxide nanoparticles and their applications for photocatalytic and antimicrobial activities

Daoiya Zouied
ch_hanine@yahoo.fr
University of Skikda
Wissame Chettah
University of Skikda
Malika Khalfoui
University of Skikda
Karima Dob
University of Skikda
Nawal Bouzenad
University of Skikda
Asma Boulahsa
University of Skikda
Hosna Bouhali
University of Skikda
Karima Derdour
University of Skikda
Nesrine Ammouchi
University of Skikda
Mohamed-Salah Medjram
University of Skikda
Emna Zouaoui
University of Skikda

Research Article

Keywords: ordinary steel, Arum italicum plant extract, anti-corrosion, Green synthesized of Ag nanoparticles, photocatalytic, antimicrobial activity

Posted Date: March 7th, 2024

DOI: https://doi.org/10.21203/rs.3.rs-4006803/v1

Additional Declarations:
No competing interests reported.

Tables 1 to 3 are available in the Supplementary Files section.

Anti-corrosion efficiency of Arum italicum root extracts, green synthesis of silver oxide nanoparticles and their applications for photocatalytic and antimicrobial activities.

Daoiya Zouied[1*]; Wissame Chettah[1]; Malika Khalfoui[1] ; Karima Dob[2]; Nawal Bouzenad[3], Asma Boulahsa[3]; Hosna Bouhali[4]; Karima Derdour[1]; Nesrine Ammouchi[4]; Mohamed-Salah Medjram[1]; Emna Zouaoui[2]

[1]Laboratory of Chemical Engineering and Environment of Skikda (LGCES), University-20 Aout-1955-Skikda, Algeria

[2] Laboratory of Stimulation and Biological and Environmental Processes, University-20 August-1955-Skikda, Algeria

[3] Laboratory of interactions, biodiversity, ecosystems and biotechnology (LIBEB), University 20 august 1955 Skikda (Algeria).

[4] Laboratory of Physico-Chemical research of Surfaces and Interfaces, University 20 Août 1955, Skikda, (Algeria).

***Corresponding author: ch_hanine@yahoo.fr**

Abstract

In this work, we used the ethanolic extract of the Arum italicum plant as a corrosion inhibitor of ordinary steel. The ethanolic extract of the Arum italicum plant is a good corrosion inhibitor of ordinary steel in a 3% HCl solution and their efficiency depends on the concentration and temperature. The electrochemical study by polarization gives an excellent efficiency of 97.85% for a concentration of 750ppm which is in good agreement with the data obtained from EIS (97.21%). The polarization curves for the steel electrode show that the extract is of mixed type. The adsorption of this inhibitor on the steel surface follows the Langmuir isotherm and physisorbed on this surface.

Green synthesized of Ag nanoparticles product shows a very significant photocatalytic activity where The photocatalytic degradation efficiency of about 98% observed for Ag NPs in the presence of 150 min of sunlight irradiations. So these observed results strongly indicate that Ag NPs are photocatalytically active under sunlight irradiation. It indicates that sunlight irradiation highly induces the photocatalytic process of Ag NPs.

The antimicrobial activity results, reveal significant inhibition diameters for different concentrations of the substance tested against E. coli, S. aureus, and P. aeruginosa. . Silver nanoparticles demonstrated efficacy against both gram (+) and gram (-) bacteria, confirming their antimicrobial potential. In addition, a reduction in microbial growth was observed with increasing nanoparticle concentration.

Keywords: ordinary steel; Arum italicum plant extract; anti-corrosion, Green synthesized of Ag nanoparticles ; photocatalytic ; antimicrobial activity.

Introduction

In recent years, nanotechnology has played an important role in the production of new materials based on metal oxides with unique physicochemical properties for versatile solicitation [1,2].

In contemplation of attaining the exclusive properties of metal oxide nanoparticles by various physical, chemical and biological synthesis routes have played a significant contribution.

These physical and chemical routes produce considerable negative impact on the environment, that involves usage of includes dangerous biological solvents, poisonous reagents, nonbiodegradable alleviating agents[3,4]. Or that reason, it is essential to the synthesis of nanoparticles by adopting feasible and safe biological methods. Due to some unique properties like simplicity, availability and stability, the plant-mediated synthesis methods were considered for the mass production of nanoparticles. Silver nanoparticles (Ag NPs) are used in many fields as alternative medicine to antibiotics, sensors, spectroscopy and catalysis, corrosion inhibition, catalysis, antimicrobial, anticancer and agriculture etc. These areas can be used in industry such as food and textile, especially in health [5,6].

The use of medicinal plants to heal originated a long time ago in traditional, Roman, Indian, Chinese, and Arab-Muslim medicine.

On the other hand, in addition to the biological activities of plants, in recent years, the attention of researchers has focused on the anti-corrosive properties of natural products of plant origin. Indeed, natural products such as compounds extracted from plants seem to be an ideal ecological alternative to replace traditional corrosion inhibitors [7].

Arum italicum is a plant belonging to the Araceae family, widely distributed in North Africa (Algeria, Morocco, and Tunisia). Their tubers and leaves are reported to be used as soap in Europe. In addition, it is consumed by the local population during a specific time of the year (beginning of winter) to avoid its toxicity. Finally, the tubers are also used to treat breast cancer, while the leaves are used as a treatment for coughs (Ethnobotanical survey not granted) [8, 9, and 10].

The ecological synthesis of nanoparticles by biological entities such as plants, algae [11], bacteria[12], fungi, and viruses[13], is considered a new simple, rapid, economical, and ecological alternative[14,15]. The use of plant extracts has several advantages such as ease of access and safe handling. It allows the production of large quantities of nanoparticles and it can act as both a reducing agent and a stabilizer in the synthesis of nanoparticles [16].

These forms of synthesis are used for several applications such as photocatalysis, antibacterial, anticancer, etc.

The important motive of this research work is to study the anticorrosion behavior of ethanolic extracts of the Arum italicum plant as well as their synthesis of Ag nanoparticles and their photocatalytic and antimicrobial activity. As in previous reports, for the first time, Ag NPs were synthesized from Arum italicum root extracts, using green synthesis for multifunctional applications. The physicochemical, structural, optical and catalytic properties were analyzed by various techniques to evaluate the anticorrosive behavior of the plant extract, photocatalytic and antimicrobial activities of the prepared Ag NPs.

Experimental

Preparation of Arum italicum root extracts

The roots of the Arum italicum were harvested in Bin El-Ouiden to the west of the wilaya of Skikda. The roots were washed several times with distilled water and then spread in the laboratory at room temperature. The dry roots were ground into powder and 20 g of powder was soaked in 400 ml of acidified ethanol water at room temperature. The filtrate was concentrated and dried to powder at 35 °C while the air-dried residue was weighed to evaluate the extract yield. The extract was labeled and stored in a laboratory cabinet at room temperature for later use.

2.3 Preparation of silver nanoparticles

The Arum italicum root extract was initially prepared at a concentration of 1000 ppm. 500 ml of extract was mixed with 1000 ml of $AgNO_3$ of concentration 1 mM at 25–30 °C, stirred regularly, and observed a color change which indicates complete bio-reduction and formation of nanoparticles. The formed nanoparticle was washed three times in distilled water, oven-dried at 35 °C, and used for subsequent analyses while the remaining colloidal solution was stored in an amber-colored reagent bottle inside the laboratory at room temperature [17].

Material preparation

The solution is the HCl 1M, The chemical composition (wt%) of carbon steel(RA1/K) electrodes used in this study was. Ti = 0, 04 %, Fe= 94.66%, Mn=0.3%, Cr=0.03% , Mo=0.03 %, V=0,03 and Ni=0,18 .

The working electrode was carbon steel (RA1/K) inserted in epoxy resin with exposed area of about $1cm^2$, abraded with emery papers (1200-250) and grease removed with acetone.

Electrochemical methods

The electrochemical studies were carried out in a cell with three electrodes, carbon steel as the working electrode, a platinum electrode as the counter electrode and a saturated calomel electrode as the reference electrode. The polarization experiments and electrochemical impedance spectroscopic investigations, EIS, were performed using a VoltalabPGZ 301 ''All-in-one" potentiostat/Galvanostat system. To achieve quasi-stationary condition, the polarization experiments were carried out using a scan rate of 10 mV /s. the potential of measure was between -1200 and -200mv. Impedance, Z, and phase shift Ɵ was recorded in the frequency domain 100KHZ at 100 mHZ.

$$E(\%) = \frac{\mathrm{Rct} - \mathrm{R°ct}}{Rct} \times 100 \quad (1)$$

Where R_{ct} and R^0_{ct} are the charge transfer resistances in the presence and absence of inhibitor, respectively.

Electrochemical parameters such as the corrosion potential (Ecorr), corrosion current (Icorr), and anodic (ba) and cathodic (bc) Tafel slopes were obtained, and the inhibition efficiency was calculated using,

$$E(\%) = \frac{(I°corr - Icorr)}{I°corr} \times 100 \quad (2)$$

Where $I°_{corr}$ and I_{corr} are the corrosion current densities without and with the inhibitor, respectively. [19, 20].

photocatalytic activity

To evaluate the photocatalytic activity of the silver nanoparticles obtained we followed the degradation of the methylene blue (BM) dye with The initial concentration of the BM solution is C0 = 7.5 ppm, 0.2 g of the photocatalyst is added to 200 mL of the MB solution in order to activate the degradation process. The variation in the concentration of the irradiated MB solution is measured after regular times by the absorbance of dyes which absorb in the visible, using UV-vis (1800 SHIMADZU) at 664 nm.

Antimicrobial activity

The antimicrobial efficacy of Ag NPs synthesized from Arum italicum against bacterial strains from the American Type Culture Collection (ATCC) was investigated. These strains included gram-positiveStaphylococcus aureus ATCC® 6538, as well as gram-negative Escherichia coli ATCC® 25922 and Pseudomonas aeruginosa ATCC® 27853. The Algerian Pasteur Institute provided all of these strains.An agar diffusion test was used to analyse the inhibition of bacterial growth by silver nanoparticles synthesised from Arum italicum. Each bacterial strain was incubated in nutrient broth for 18 hours at a temperature of 37°C. The bacterial isolats' inoculums were prepared aseptically, and the cell density was adjusted to 106 CFU/mL, or 0.55 McFarland standard, in order to uniformly reseed the Agar Muller Hinton plates using a sterile swab. The silver/PG nanoparticles were serially diluted starting at 2048 µg/mL and subsequently diluted to 1024, 512, 256, 128, 64, and 32 µg/mL.The disks were placed in the designated location on the gelfilled medium and they were impregnated with varying concentrations of the nanoparticle solution, using 30 µL of each solution. After 24 hours of incubation at 37 °CPetri dishes were collected, zones of inhibition formed around the discs were checked, and measurements of these zones were taken.

RESULTS AND DISCUSSION

Characterization of arum italicum(AI) extract and synthesized Ag NPs/AI

Figure 1 shows the UV–vis spectra of the AI plant extract and Ag NPs/AI. a peak was observed at 333.5 in the UV-vis spectrum of the AI plant extract, whereas for Ag NPs/AI, it was observed that the maximum signal completely disappeared at 670 nm and the signal intensity around 406,5 nm was considerably reduced, however in the literature the AgNO3 (Ag^{+1}) solution gave two peaks at 670 and 405 nm in the UV-vis spectrum. This can be interpreted as a substantial reduction of the cation Ag^{+1} in metallic silver [21, 22].

The XRD diffraction pattern of Ag NPs/AI is presented in Figure 2. The peaks observed for 2θ values = 37°, 48°, 67°, and 78°, correspond to (111), (200), (220), and (301) lattice planes of the face-centered cubic structure of AgNPs.It is understood that these values are quite compatible with the reference data[23].

Determination of anticorrosion activity of arum italicum root extract

Polarization curves

Figure .3. Presents the polarization curves for RAI/K steel in 1M HCl solution in the absence and presence of different extract concentrations at 25°C.

On the representation log I = f(E) , we distinguish two parts for each curve. A cathodic part that corresponds to the reduction reaction of oxygen on the surface of the steel, and an anodic part that represents the oxidation reaction. The values of corrosion current density (i_{corr}), corrosion potential (E_{corr}), cathodic and anodic Tafel slopes (Bc and Ba), inhibition efficiency E (%), and recovery rate (θ) for different concentrations of extracts are collected in the table 1. The inhibitory efficiency (E %) is given by the equation (1).

The analysis of data shown in Table 1 clearly shows that the corrosion current densities (I_{corr}) decrease as the extract concentration increases and that the inhibitory efficiency E(%) increases with the increase in the inhibitor concentration to reach a maximum of 97.85% for 750ppm. Beyond 750ppm, we notice a decrease in inhibitory efficiency.

The addition of the extract to the corrosive medium causes a modification of the values of the Tafel slopes, indicating that both anodic and cathodic reactions are affected. In the presence of the extract, the corrosion potential shifts towards positive values. According to Ferreira et al[24]. And Li et al[25], if the corrosion potential in the presence of the inhibitor shifts by a value greater than 85 mV relative to the blank, the inhibitor can be considered as an anodic or cathodic inhibitor. In our case, the variation in potential is less than 85mV. This result leads us to say that the extract is a mixed type inhibitor.

Electrochemical impedance spectroscopy

Electrochemical impedance is a powerful tool in the study of corrosion and adsorption phenomena [26,27]. It was studied with the aim of completing the understanding of the corrosion and inhibition mechanisms of steel in 1M HCl medium.

Figure .4 represents the impedance and Bode diagrams in the absence and presence of different extract concentrations at 298 K.

We notice that:
For 0ppm inhibitor (without inhibitor) and with the different concentrations, an increase in the size of the semi-circle capacitive loops. The latter is reflected by the double layer capacitance and transfer resistance (Rct). Only one time constant is detected, this can be attributed to the frequency dispersion of the inter-facial impedance. The equivalent circuit giving the response of the electrochemical interface is presented in figure 5.
The charge transfer resistance (Rt) value obtained in the absence of an inhibitor testifies to the steel dissolution from the first hours of immersion, this is generally attributed to a conductive layer of corrosion products [28]. The extract concentration increasing results in an increase in the charge transfer resistance (Rtc) and a reduction in the double layer capacitance (Cdl) until a maximum concentration is obtained of 750ppm. This is the result of the protective film formation on the metal surface. The decrease in Q may be related to the decrease in the dielectric constant and/or the increase in the thickness of the double layer **[29].** In other words, in the presence of inhibitors, the thickness of the double layer decreases and by changing the oxide layer, the value of Q decreases **[30-31].**

The improvement in film properties is characterized on the impedance diagram by an increase in the size of the loops.After calculation, we obtain a maximum efficiency value which is 97.21% for 400ppm of the extract.

Adsorption isotherms

The inhibition of metal corrosion by organic compounds is explained by their adsorption on the metal surface. Adsorption isotherms are then an important complement capable of determining the mode of these organic compounds' adsorption on the surface. In order to obtain the isotherm, the metal surface coverage rate of the metal surface as a function of the inhibitor concentration must be obtained **[32].**

To identify the adsorption type corresponding to the present study, different types of isotherms were tested. According to these isotherms, the recovery rate (Θ) is linked to the concentration of C_{inh} inhibitor by the following equations:

$$\theta = \frac{bC_{inh}}{1 + bC_{inh}} \qquad \text{(Isotherme de Langmuir)} \quad (3)$$

$$\exp(-2a\theta) = KC_{inh} \qquad \text{(Isotherme de Temkin)} \quad (4)$$

$$\left(\frac{\theta}{1+\theta}\right)\exp(2a\theta) = KC_{inh} \qquad \text{(Isotherme de Frumkin)} \quad (5)$$

b: Adsorption coefficient, K: Equilibrium constant of the adsorption process

a: Interaction constant between adsorbed particles, Cinh: Concentration of the inhibitor.

Based on the R^2 values, we can conclude that the Langmuir model is the most verified where the correlation coefficient is 0.99. The slope of the curve is different in the unit. We can explain this discrepancy based on the interaction between the molecules adsorbed on the metal surface by the forces of attraction or repulsion **[33].**

The equilibrium constant K_{ads} is linked to the standard adsorption free energy (ΔG^0_{ads}) by the following equation:

$$K_{ads} = \frac{1}{55.5}\exp\left(\frac{-\Delta G^0_{ads}}{RT}\right) \ldots\ldots\ldots\ldots\ldots\ldots\ldots\ldots\ldots\ldots\ldots\ldots\ldots\ldots\ldots\ldots\ldots\ldots\ldots\ldots. (6)$$

R: Ideal gas constant, T: Temperature, 55.5: Concentration of water in solution (mole. l^{-1}).

After calculation, we obtain a value of ΔG^0_{ads} equal to -9.9024KJ / mol. ΔG^0_{ads} Negative values indicate that the inhibitor molecules' adsorption on the metal surface is spontaneous.

Several researchers think that for values of ΔG^0_{ads} close to –20 kJ /mol, this corresponds to the electrostatic interactions between charged molecules and the metal charges (physisorption), on the other hand, when ΔG^0_{ads} is close to –40 kJ/mole, it corresponds to a transfer of charges between the inhibitor molecules and the metal surface by forming covalent bonds (chemisorption) **[33;34].**

In the present work, the calculated ΔG^0_{ads} values are slightly less negative than -20kJ mol^{-1}, which indicates that the inhibitor molecules' adsorption is done by physisorption.

photocatalytic activity of synthesized Ag NPs/AI

Equilibrium time curve

Figure 6 present the Equilibrium time curve, before irradiation, the system is placed in a dark room to optimize the adsorption/desorption equilibrium time.

We notice that the system equilibrium time is 30 min. once the adsorption equilibrium is reached, radiation must be started. The photocatalytic test of material synthesized during this study consists of monitoring the concentration degradation of BM in aqueous solutions under irradiation with visible light.

The photo-degradation efficiency is calculated by the following equation:

$$efficiency\ degradation(\%) = \frac{C_0 - C}{C_0} \times 100$$

Figure 7 shows the evolution of the degradation activity measured in the absence and presence of green catalyst as a function of time.

The time-dependent absorption spectra of the prepared photocatalyst are shown in Fig. 6. A strong typical absorption peak at 664 nm corresponds to BM dye, which decreases with the increase of irradiation time (00, 10, 20, 30, and 60 min) in the presence of Ag NPs. The photocatalytic degradation efficiency of about 98% observed for Ag NPs in the presence of 150 min of sunlight irradiations. So these observed results strongly indicate that Ag NPs are photocatalytically active under sunlight irradiation. It indicates that sunlight irradiation highly induces the photocatalytic process of Ag NPs.

Antimicrobial activity

The antimicrobial activity results, presented in Table 3, reveal significant inhibition diameters for different concentrations of the substance tested against E. coli, S. aureus, and P. aeruginosa. Maximum inhibition diameters were recorded at 20.33 mm for E. coli, 20.75 mm for S. aureus, and 20.66 mm for P. aeruginosa, all at a concentration of 2048 µg/Ml (Figure 8). These observations indicate a dose-dependent trend, highlighting increased antimicrobial activity with higher concentrations of the substance. Silver nanoparticles demonstrated efficacy against both gram (+) and gram (-) bacteria, confirming their antimicrobial potential. In addition, a reduction in microbial growth was observed with increasing nanoparticle concentration, as previously reported [**35**] .These promising results suggest a strong antimicrobial potential of the substance, surpassing the performances obtained in other studies on the antimicrobial potential of Ag NPs synthesised using Arum italicum **[36,37]**.

Conclusion

The anticorrosion study was carried out using electrochemical methods such as impedance spectroscopy (EIS) and polarization curve. The results obtained are:

- ✓ The ethanolic extract of the Arum italicum plant is a good corrosion inhibitor of RA1/K steel in a 3% HCl solution and their effectiveness depends on the concentration and temperature.
- ✓ The best inhibition efficiency obtained from the polarization curves is: 97.85% at 750ppm and 97.21 from EIS.
- ✓ The results obtained from the polarization curves are in good agreement with the data obtained by EIS.
- ✓ Polarization measurements indicate that Arum italicum extract is a mixed type inhibitor.
- ✓ The green synthesis of silver nanoparticles yields a good amount of synthesized product.

The photo degradation of BM as a function of irradiation time is shown that, in the presence of catalyst, approximately 80% of the BM solution degrades after 60 min, and almost completely disappears after 150 min. The antimicrobial activity results reveal significant inhibition diameters for different concentrations of the substance tested against E. coli, S. aureus, and P. aeruginosa. . Silver nanoparticles demonstrated efficacy against both gram (+) and gram (-) bacteria, confirming their antimicrobial potential. In increasing addition, a reduction in microbial growth was observed with nanoparticle concentration.

Declarations of interest

The authors declare no conflict of interest in this reported work.

Acknowledgement

We gratefully acknowledge the Laboratory Engineer Ladacia Sana for his participation in carrying out my work at the research laboratory level (LGCES), University-20 August-1955-Skikda, Algeria.

References

[1] R. Medhi, M.D. Morquez, T.R. Lee, A.C.S. Appl, Nano Mater. 3 (7) (2020) 6156–6185, https://doi.org/10.1021/acsanm.0c01035.

[2] V. Kavitha, P. Mahalingam, M. Jeyanthinath, N. Sethupathi, Mater. Today-Proc.23 (2020) 12–15, https://doi.org/10.1016/j.matpr.2019.05.351.

[3] V. Kavitha, P. Mahalingam, M. Jeyanthinath, N. Sethupathi, Mater Today-Proc. 35 (2021) 48–52, https://doi.org/10.1016/j.matpr.2019.05.437.

[4] H. Qin, Q. Wei, J. Wu, F. Yang, B. Zhou, Y. Wang, S. Tian, Mater. Chem. Phys. 232 (2019) 240–245, https://doi.org/10.1016/j.matchemphys.2019.04.081.

[5] Pandit R. Nusantara Biosci. 2015;7(1):15-19.

[6] Rai M, Yadav A, Gade A.. Biotechnol Adv. 2009;27(1):76- 83.

[7] Mori, Y.; Ono, T.; Miyahira, Y.; Nguyen, V.Q.; Matsui, T.; Ishihara, M. Nanoscale Res. Lett. 2013, 8, 93.

[8] Hale Gamze Ağalar , Gülşen Akalın Çiftçi , Fatih Göger and Neşe Kırımer. Rec. Nat.Prod. 12:1 (2018) 64-75

[9] Oğuz Ayhan Kireçci , Zehra Gökçe , Ayşe Dilek Özşahin Kireçci , Gülcan Balcı , Ökkeş Yılmaz. Journal of Science and Technology. ISSN 2146-7706 2, (2012),52-56.

[10] M.M. Haneefa, M. Jayandran, V. Balasubramanian, Asian J. Pharm. 11 (2017) 65–74.

[11] K. Govindaraju, S. KhaleelBasha, V. Ganesh Kumar, G. Singaravelu, Materials Sci. 43 (2008) 5115-5122.

[12] M.F. Lengke, M.E. Fleet, G. Southam, Langmuir. 23 (2007) 2694–2699.

[13] D. Rautaray, A. Ahmad, M. Sastry, Am. Chem. Soc. 125 (2003) 14656–14657.

[14] A. Saxena, R.M. Tripathi, R. P. SINGH, Dig. J. Nanomater.Biostruct. 5 (2010) 427–432.
[15] Amit Kumar Mittal, Yusuf Chisti, Uttam Chand Banerjee, Biotechnol.Adv.31 (2013) 346-356.
[16] S. P.Chandran, M.Chaudhary, and al, Biotechnol. Prog. 2(2006) 577–583.
[17] Ekemini Ituen, Ambrish Singh, Lin Yuanhua, Onyewuchi Akaranta. SN Applied Sciences. https://doi.org/10.1007/s42452-021-04670-w.
[18] Daoiya Zouied ,Emna Zouaoui, Karima Dob , Olfa Chikha, Hajer Fadhil. Current Topics in Electrochemistry. Vol. 24, 2022, 37 – 50.
[19] M. Behpour, S.M. Ghoreishi, N. Soltani, M. Salavati-Niasari, M. Hamadanian, A. Gandomi, Corros. Sci. 50 (2008) 2172–2181.
[20] I. El Ouali, B. Hammouti, A. Aouniti, Y. Ramli, M. Azougagh, E.M. Essassi, M. Bouachrine, J. Mater. Environ. Sci. 1 (2010)1–8.
[21] Lopes JMS, Moreira SGC, Neto, and NMB. J Braz Chem Soc. 2019;31(1).
[22] Hamdullah Seçkin, Ismet Meydan. Braz. J. Pharm. Sci. 2022;58: e20992).
[23] Liu H, Wang M, Zhang X, Ma J, Lu G. Appl Catal B: Environmental. 2018; 237(5):563-573.
[24] E. S. Ferreira, C. Giancomelli, F. C. Giacomelli and A. Spinelli, (2004). Materials Chemistry and Physics. Vol 83, pp. 129-134.
[25] Li. W.H, He. Q, Zhang. S.T, Pei. C.L, B.R. (2008). Journal of Applied Electrochemistry. Vol 38, pp. 289–295.
[26] Macdonald. J.R. (1987)," Impedance Spectroscopy". third ed. John Wiley& Sons, New York.
[27] Aït Aghzzaf A, Rhouta. B, Rocca. E, Khalil. A, Steinmetz. J.(2013). Corrosion science. Vol 80, pp. 46-52.
[28] F.Depenyou, A. Doubla, S. Laminsi, D. Moussa, J.L. Brisset.(2008). Corrosion Science. Vol 50, pp. 1422-1432.
[29] G. Mu, X. Li, G. Liu.(2005). Corrosion Science.Vol 47, pp. 1932.1952.
[30] T. Zhao, G. Mu. (1999). Corrosion Science. Vol 41, pp. (1999) 1937-1944.
[31] B. Zhang, C. He, X. Chen, Z. Tian, F. Li. (2015).Corrosion Science. Vol 90, pp. 585-596.
[32] Al-Sabagh. A, M, Migahed .M. A, Awad H. S.(2006), Corrosion. Science.Vol. 48, pp. 813.
[33] S. Deng, X. Li, H. Fu. (2011). Corrosion Science. Vol 53, pp. 822–828.
[34] S. Safak, B. Duran, A. Yurt, G. Türkoğlu. (2012) .Corrosion Science. Vol 54, pp. 251–259.
[35] Garima Singhal, Riju BhaveshKunal Kasariya,Ashish Ranjan Sharma, Rajendra Pal Singh. J Nanopart Res (2011) 13:2981–2988.
[36] Ismet Meydan, Hakan Burhan, Tuğba Gür, Hamdullah Seçkin, Bahareh Tanhaei , Fatih Gürçağ Şen. Environmental Research (2022), Volume 204, Part D, March 2022, 112363.
[37] Hamdullah Seçkin, Ismet Meydan. Braz. J. Pharm. Sci. 2022;58: e20992

Figures

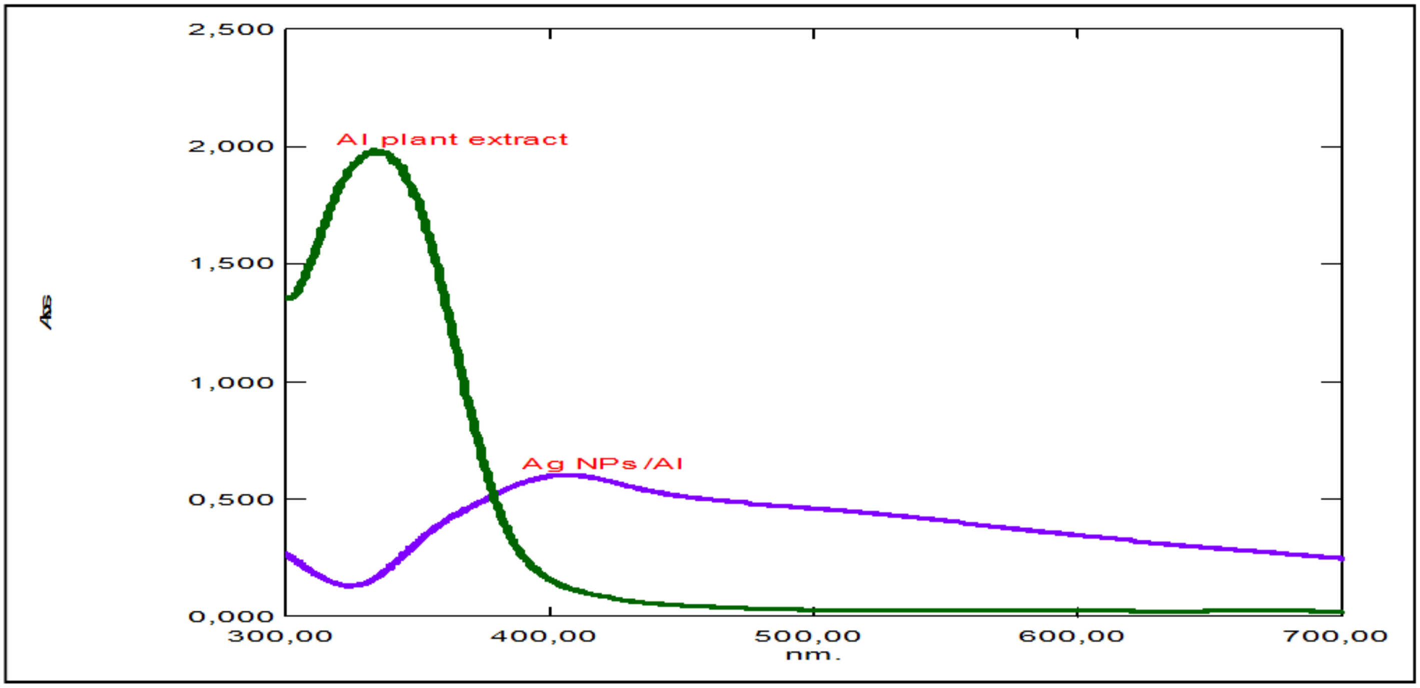

Figure 1

UV-vis spectra of AI plant extract and Ag NPs/AI.

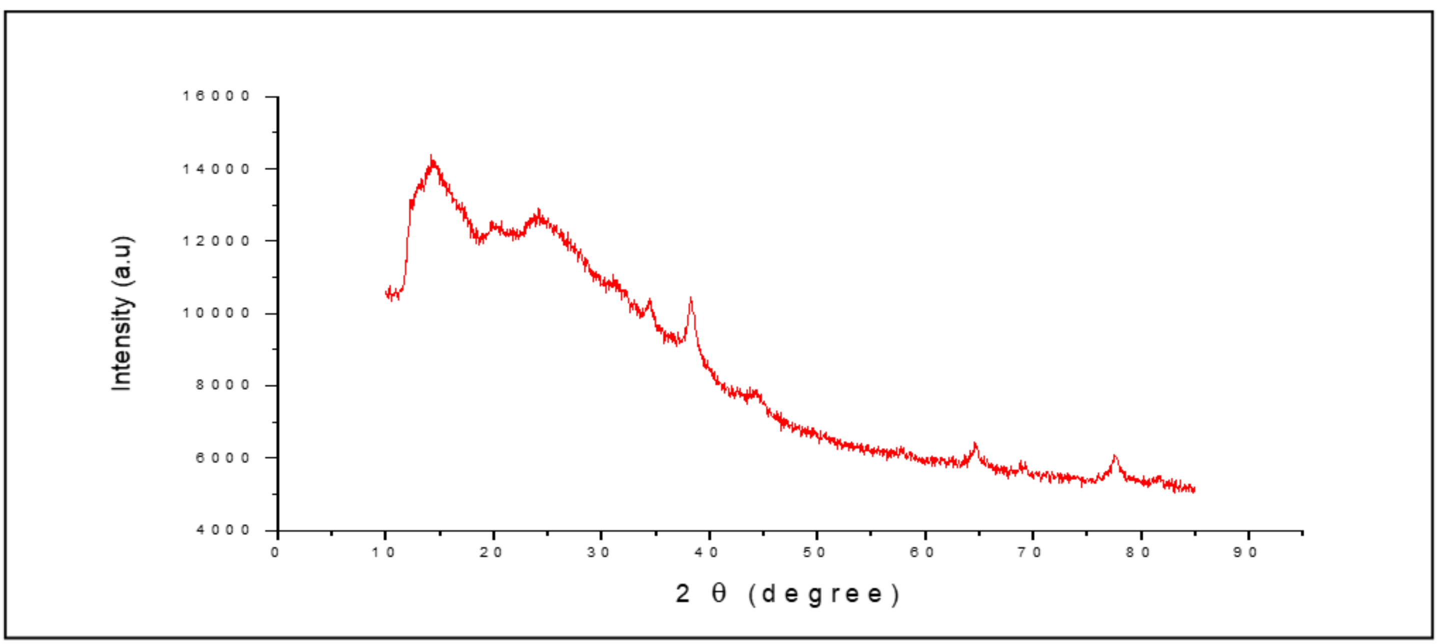

Figure 2

XRD pattern of Ag Nps/AI.

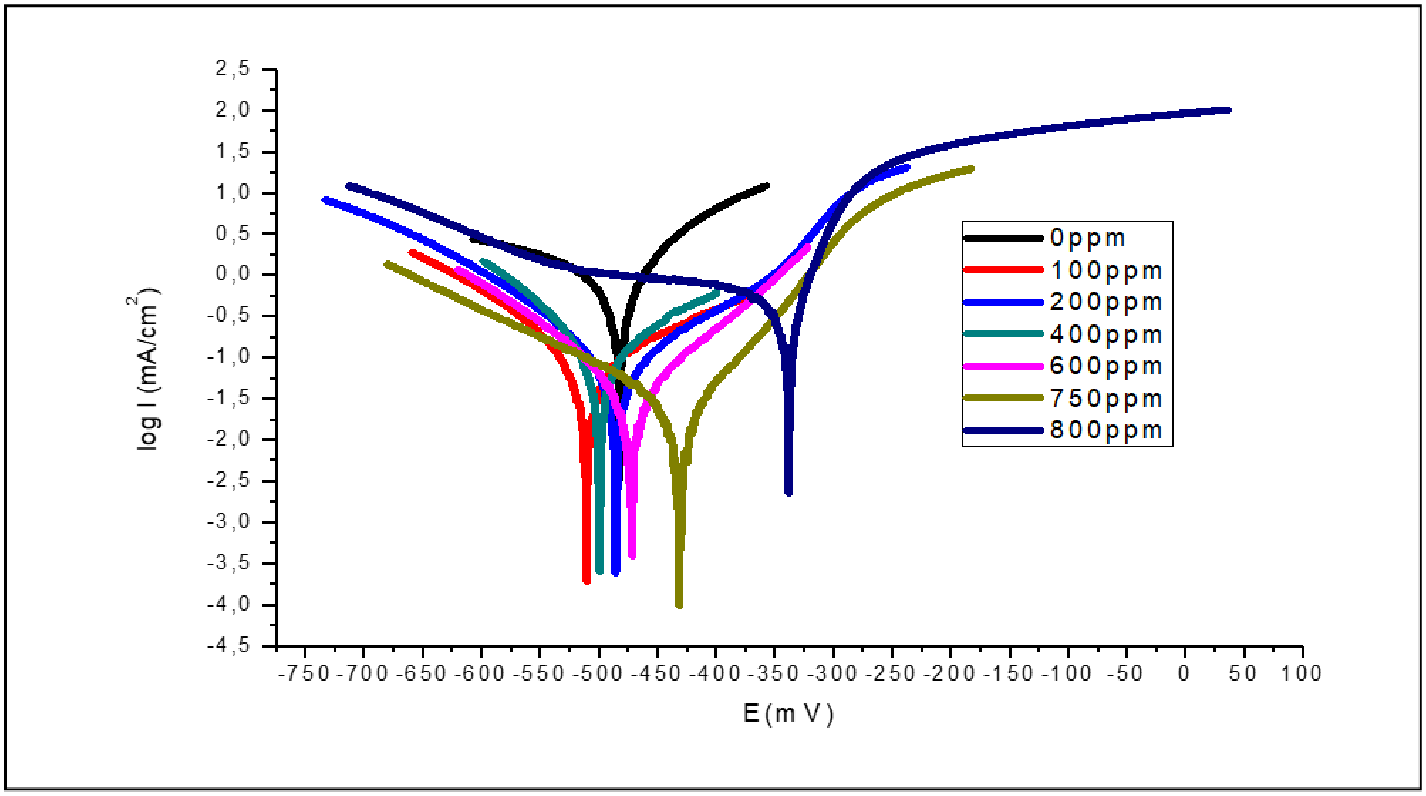

Figure 3

The polarization curves of RAI/K steel in 1M HCl in the absence and presence of different concentrations of arum italicum extracts at 25°C.

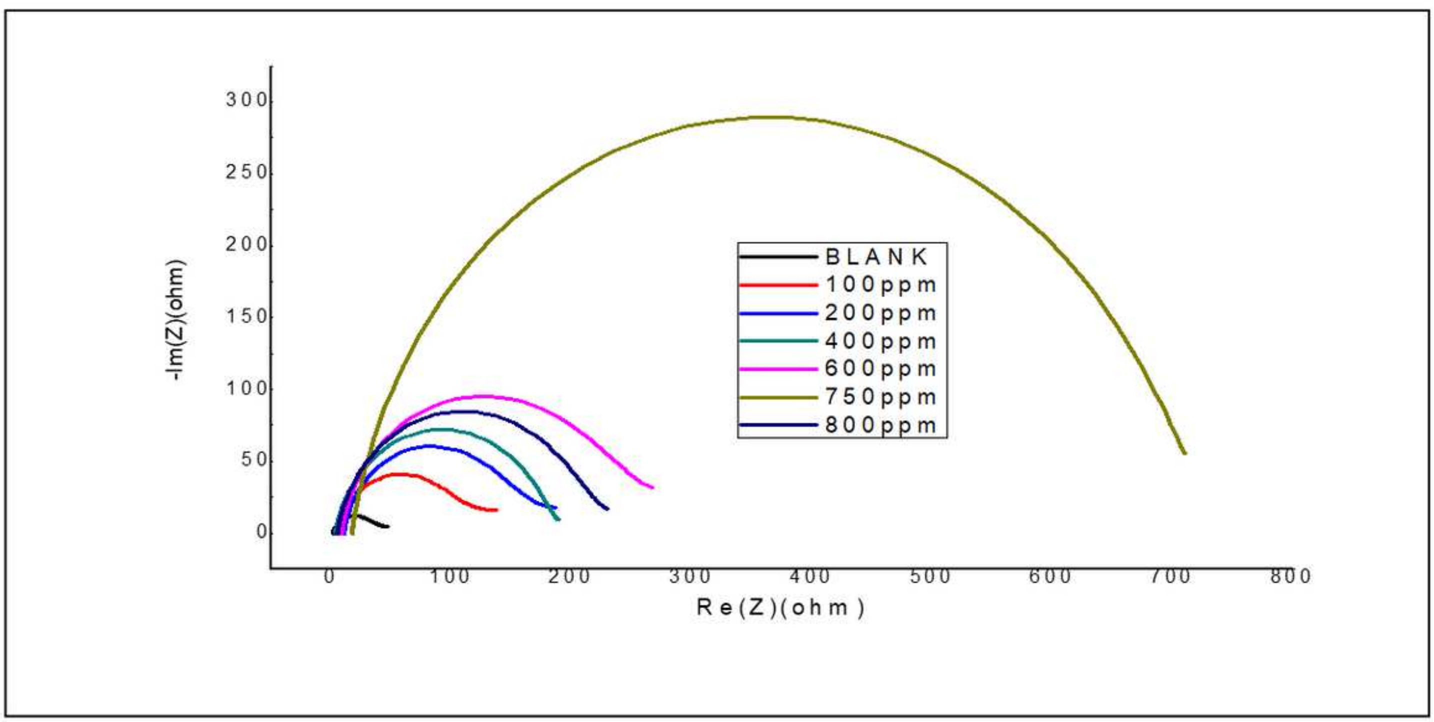

Figure 4

Nyquist diagrams without and with different concentrations of arum italicum extracts at 25°C.

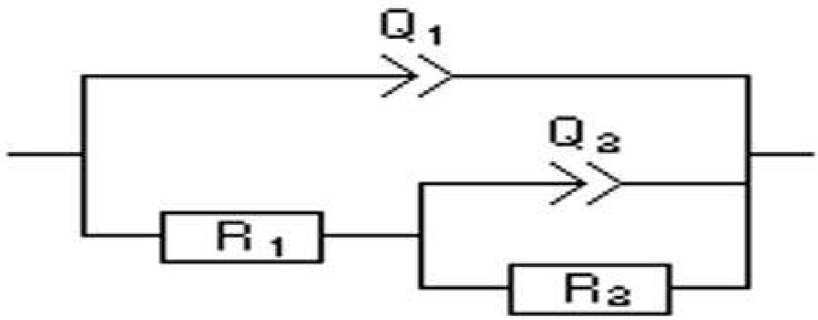

Figure 5

The equivalent circuit simulates the impedance data for steel without and with different extract concentrations at 25°C.

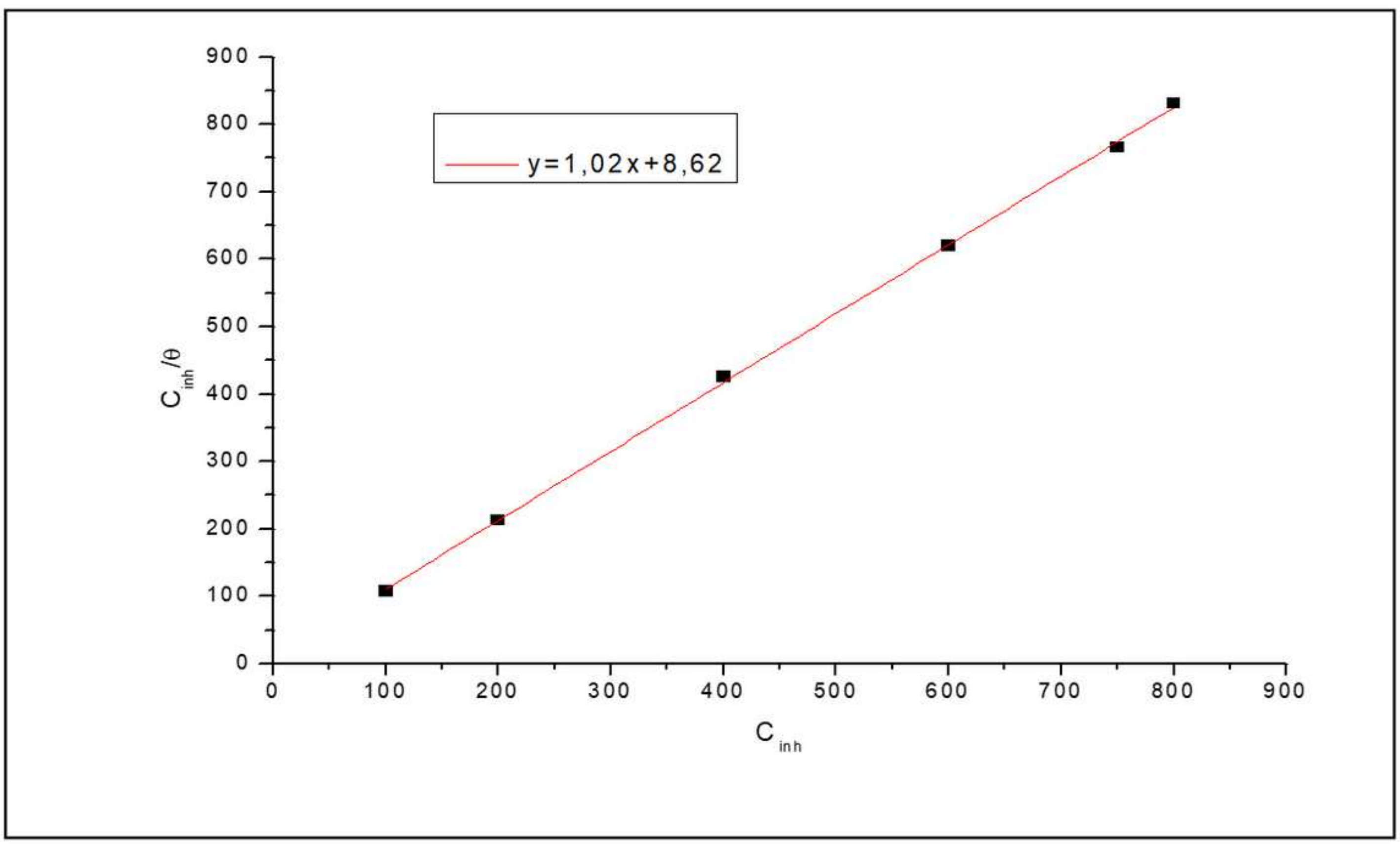

Figure 6

Figure 5 Langmuir adsorption isotherm for steel with different concentrations of arum italicumextracts at 25°C.

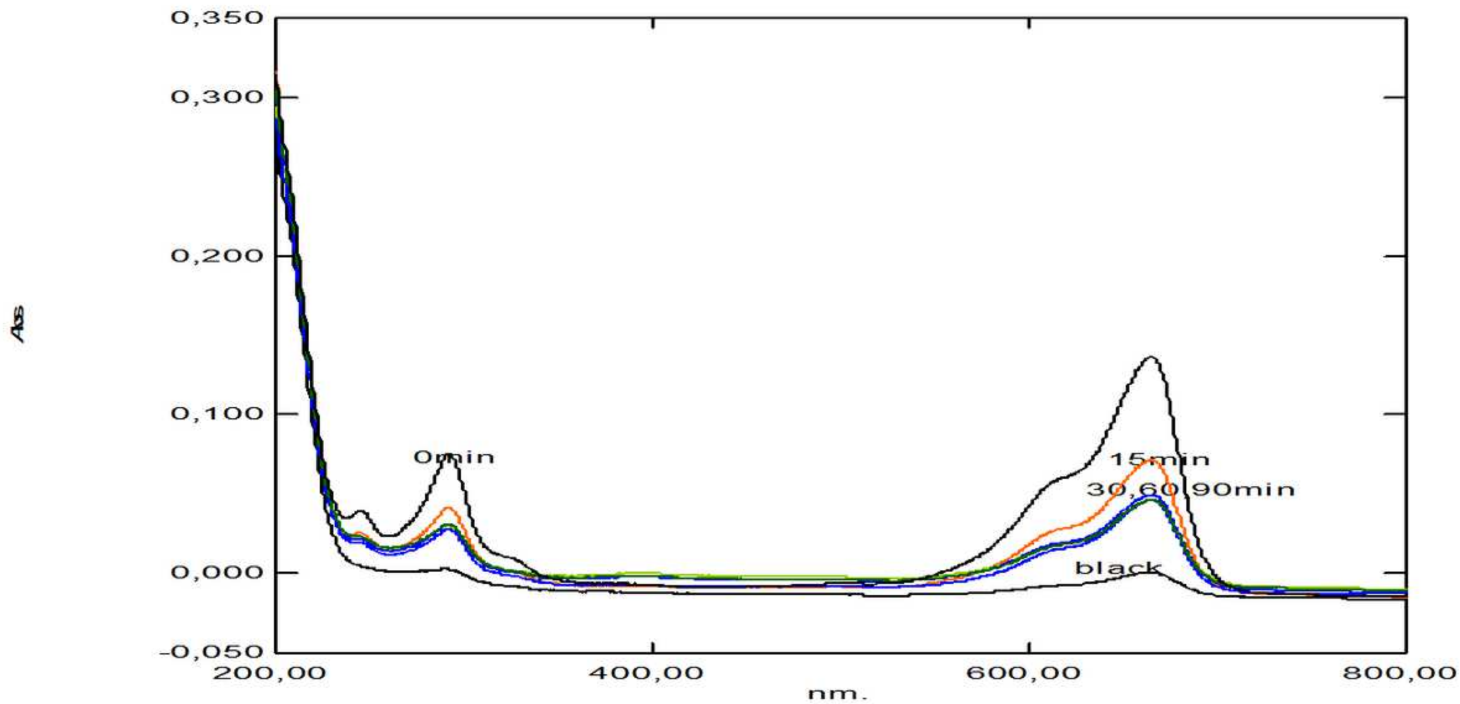

Figure 7

Figure 6. The Equilibrium time curve

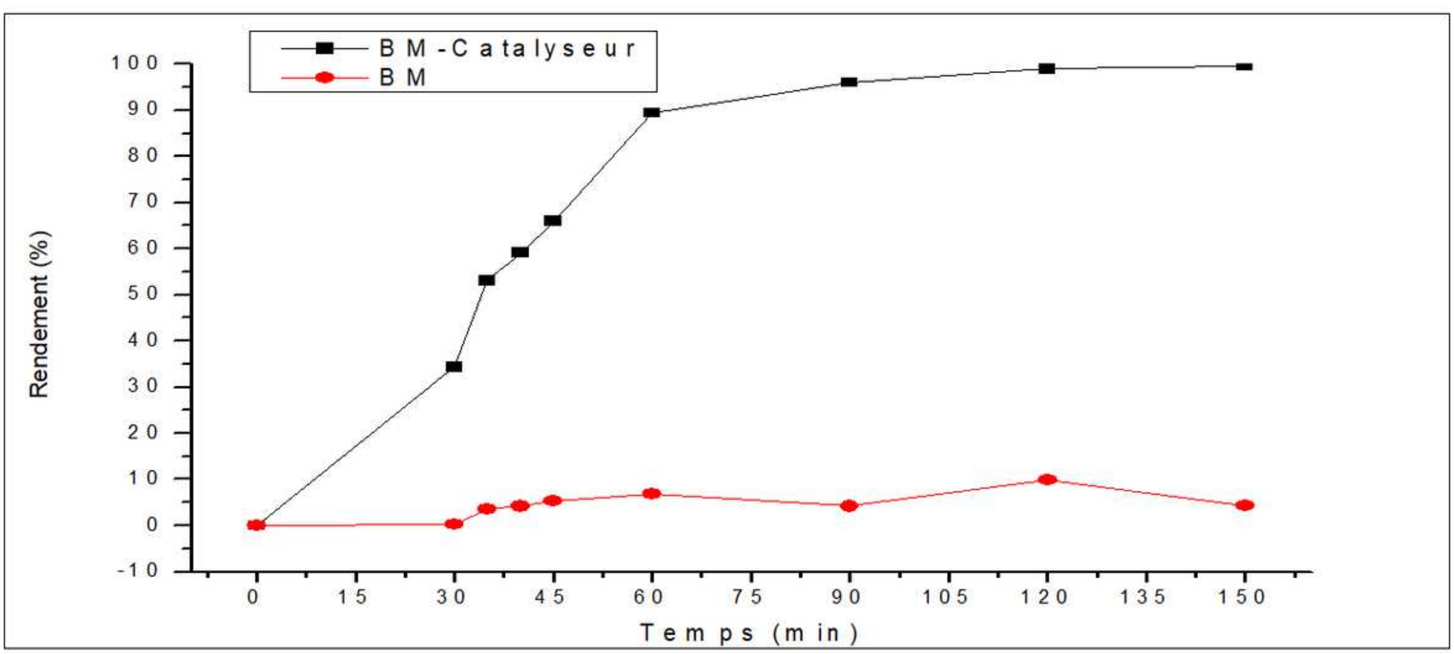

Figure 8

Figure 7. MB degradation rate with and without Catalyst

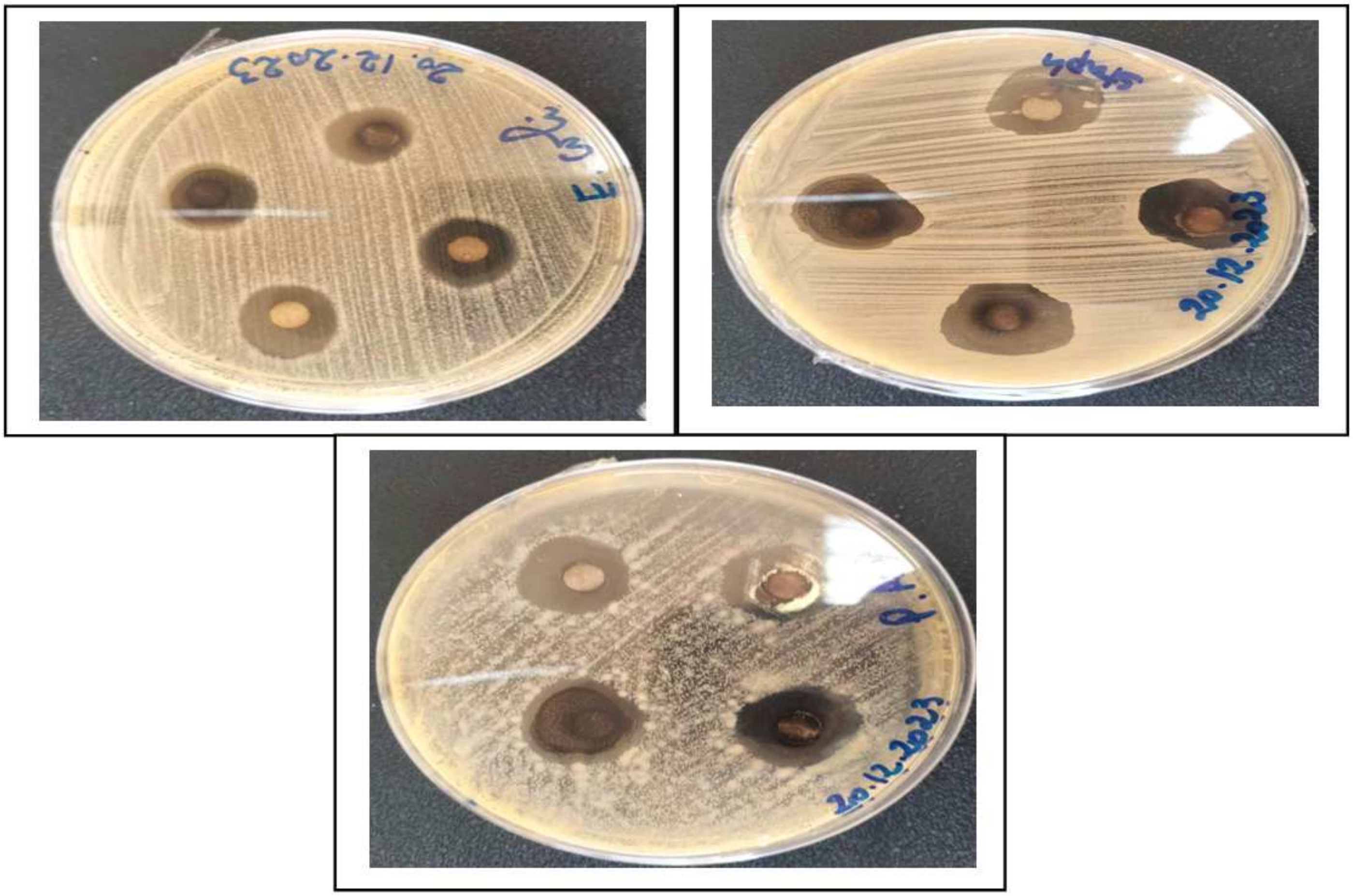

Figure 9

Figure. 8. Some images obtained by the disk diffusion method

Supplementary Files

This is a list of supplementary files associated with this preprint. Click to download.

- GRAPHICALABSTRACT.bmp
- Tablespourarticle4.docx